Cancer Cell, Volume *37*

Supplemental Information

SETD5-Coordinated Chromatin Reprogramming Regulates Adaptive Resistance to Targeted Pancreatic Cancer Therapy

Zhentian Wang, Simone Hausmann, Ruitu Lyu, Tie-Mei Li, Shane M. Lofgren, Natasha M. Flores, Mary E. Fuentes, Marcello Caporicci, Ze Yang, Matthew Joseph Meiners, Marcus Adrian Cheek, Sarah Ann Howard, Lichao Zhang, Joshua Eric Elias, Michael P. Kim, Anirban Maitra, Huamin Wang, Michael Cory Bassik, Michael-Christopher Keogh, Julien Sage, Or Gozani, and Pawel K. Mazur

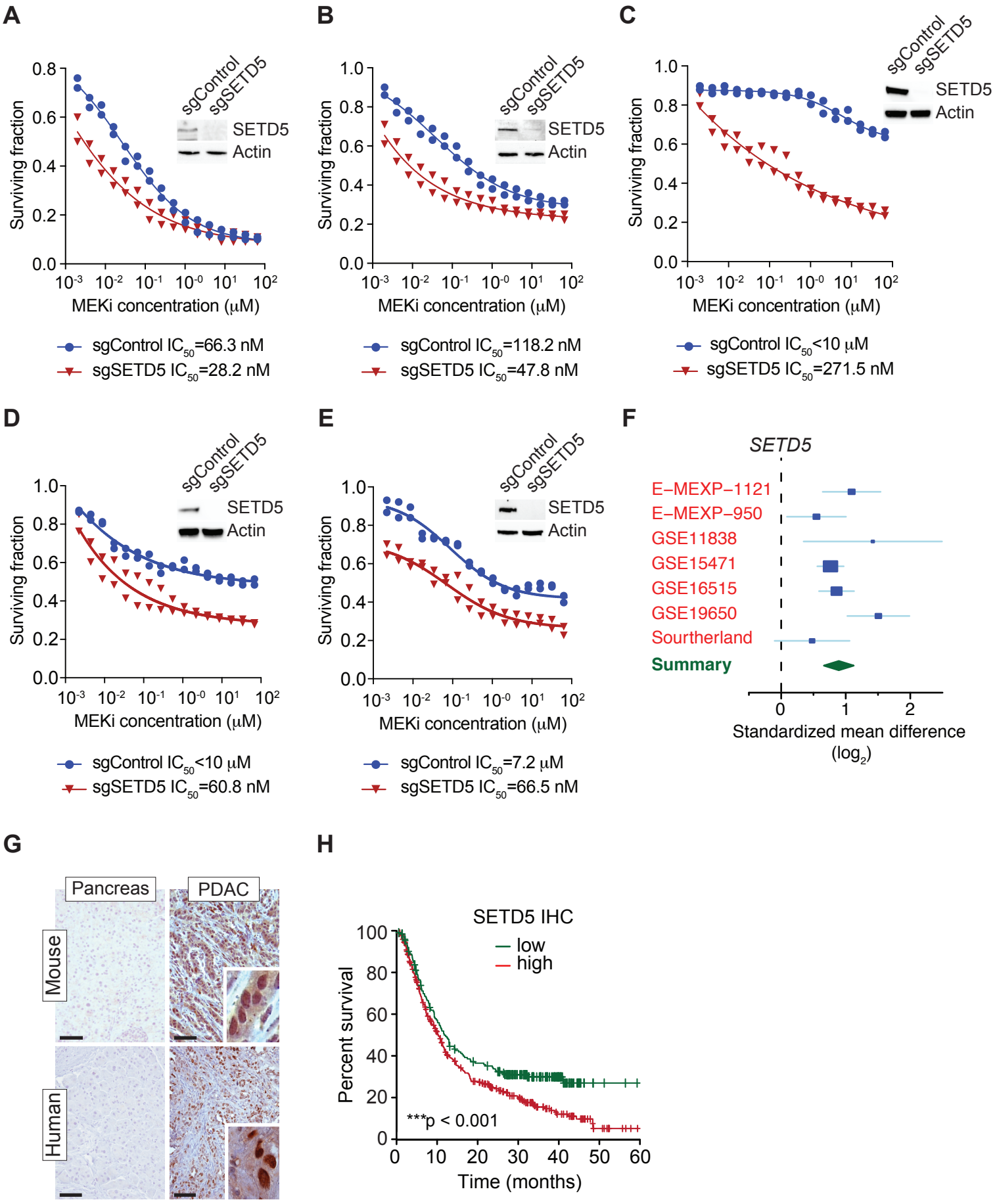
A
B
C
D
E
F
G
H
Surviving fraction
MEKi concentration (μM)
sgControl
sgSETD5
SETD5
Actin
sgControl IC50=66.3 nM
sgSETD5 IC50=28.2 nM
sgControl IC50=118.2 nM
sgSETD5 IC50=47.8 nM
sgControl IC50<10 μM
sgSETD5 IC50=271.5 nM
sgControl IC50<10 μM
sgSETD5 IC50=60.8 nM
sgControl IC50=7.2 μM
sgSETD5 IC50=66.5 nM
SETD5
E–MEXP–1121
E–MEXP–950
GSE11838
GSE15471
GSE16515
GSE19650
Sourtherland
Summary
Standardized mean difference
(log2)
Pancreas
PDAC
Mouse
Human
SETD5 IHC
low
high
Percent survival
***p < 0.001
Time (months)

Supplementary Figure 1. SETD5 expression increases in MEKi resistance and is associated with poor survival outcomes in pancreatic cancer. Related to Figure 1.

(A-E) SETD5 ablation in human PDAC cell lines CaPan1 (A), PNS1 (B), YAPC (C), DANG (D), KP4 (E) causes the shift in cellular viability in response to MEKi (trametinib) at the dose indicated on the x-axis. Geometric mean half-maximum inhibitory concentration (IC_{50}) values for MEKi calculated. Data are represented as mean ± SEM of three technical replicates in two independent experiments. Western analysis with the indicated antibodies of cancer cell transduced with Cas9 and sgRNA targeting SETD5 (sgSETD5) and a control non-targeting sgRNA (sgControl). Actin served as loading control.

(F) Summary of *SETD5* expression levels in six publicly available expression data sets of PDAC (n = 294 tumors and n = 141 normal tissue independent samples). Detailed statistical description in **STAR Methods**.

(G) Representative immunohistochemical (IHC) images showing nuclear SETD5 expression in pancreatic cancer but not in normal pancreas samples from human pancreatic cancer samples (representative of 12 independent samples) and *Kras;p53* mutant mouse model of PDAC (representative of 8 independent samples). Scale bars, 100 μm; insets present higher magnification.

(H) Analysis of correlation of SETD5 staining and PDAC patient survival assessed by IHC. ***$p < 0.001$, log-rank test, 172 different samples were stained in total.

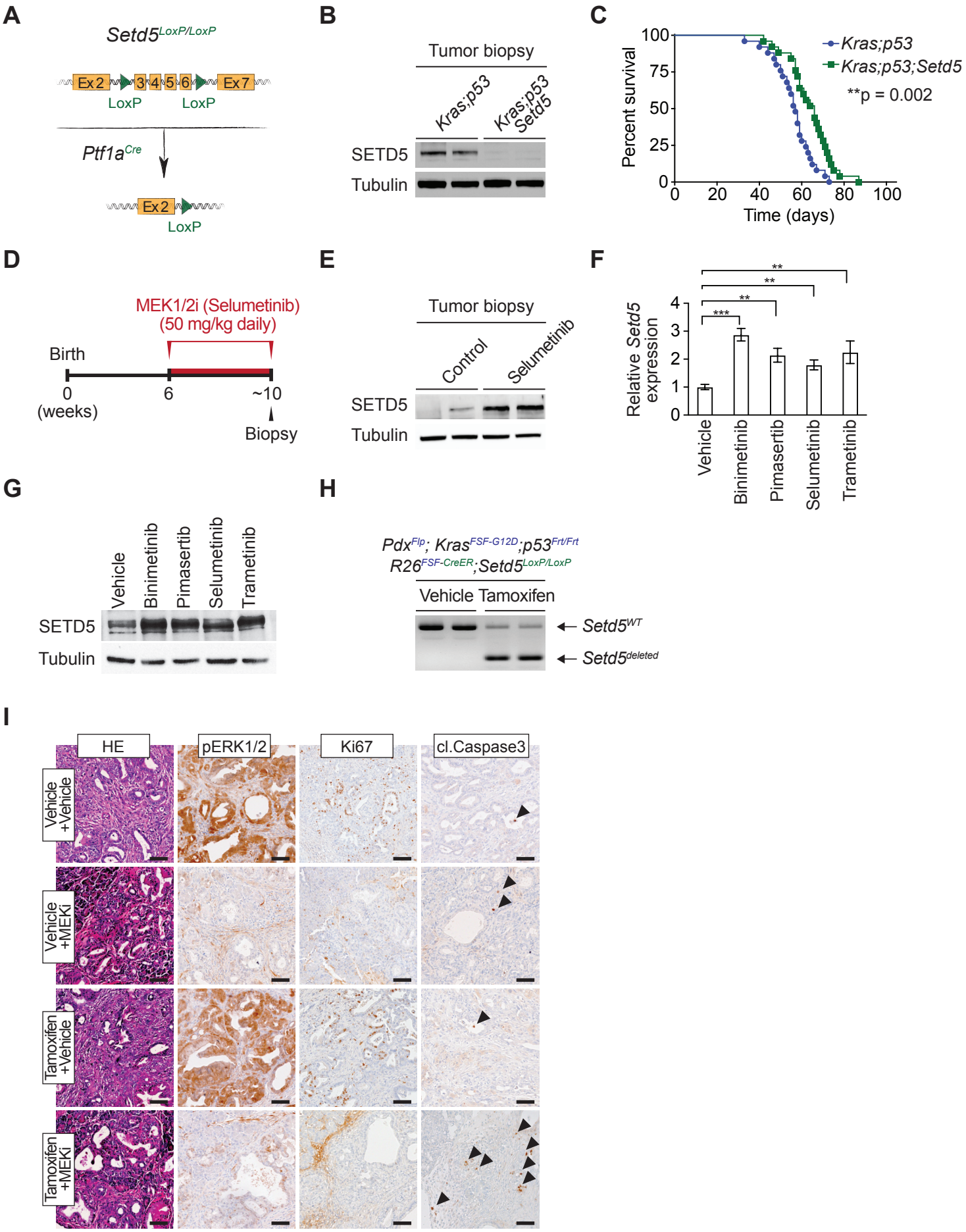
A
Setd5LoxP/LoxP
Ex 2
3
4
5
6
Ex 7
LoxP
LoxP
Ptf1aCre
Ex 2
LoxP
B
Tumor biopsy
Kras;p53
Kras;p53 Setd5
SETD5
Tubulin
C
Kras;p53
Kras;p53;Setd5
**p = 0.002
Percent survival
Time (days)
D
MEK1/2i (Selumetinib)
(50 mg/kg daily)
Birth
0
(weeks)
6
~10
Biopsy
E
Tumor biopsy
Control
Selumetinib
SETD5
Tubulin
F
Relative Setd5 expression
Vehicle
Binimetinib
Pimasertib
Selumetinib
Trametinib
G
Vehicle
Binimetinib
Pimasertib
Selumetinib
Trametinib
SETD5
Tubulin
H
PdxFlp; KrasFSF-G12D;p53Frt/Frt
R26FSF-CreER;Setd5LoxP/LoxP
Vehicle
Tamoxifen
Setd5WT
Setd5deleted
I
HE
pERK1/2
Ki67
cl.Caspase3
Vehicle +Vehicle
Vehicle +MEKi
Tamoxifen +Vehicle
Tamoxifen +MEKi

Supplementary Figure 2. Loss of *Setd5* attenuates Kras^{G12D}-driven pancreatic tumorigenesis *in vivo* and sensitizes PDAC to MEKi toxicity. Related to Figure 2.

(A) Schematic of the *Setd5* conditional allele. In the presence of Cre recombinase, exon 3 is deleted to disrupt *Setd5* expression.

(B) Western blots with the indicated antibodies of pancreatic tissue lysates from *Kras;p53;Setd5* and *Kras;p53* (control) mutant mice. Two independent and representative samples are shown for each genotype. Tubulin is shown as a loading control.

(C) Kaplan-Meier survival curves of *Kras;p53;Setd5* (n = 24, median survival = 66 days) and *Kras;p53* (control, n = 27, median survival = 57 days) mice, *p = 0.002 by log-rank test for significance.

(D) Treatment schedule for administration of Selumetinib (MEK inhibitor) or placebo (vehicle) to *Kras;p53* mutant PDAC mouse model.

(E) Western analysis with the indicated antibodies of tissue biopsy collected from *Kras;p53* mutant mice treated with Selumetinib (E), or placebo (vehicle). Two independent and representative samples are shown.

(F) Quantitative real-time qPCR (qRT-PCR) analysis of *SETD5* expression in control (vehicle) and PDAC cell lines cultured to be resistant to Binimetinib, Pimasertib, Selumetinib and trametinib. Error bars represent mean ± SD from three independent experiments, **p < 0.05, *** p < 0.001, n.s., not significant, by two-tailed unpaired Student's t test.

(G) Western blot analysis of SETD5 expression in cells in (F). A representative sample for each condition is shown. Detailed cell treatment condition description in **STAR Methods**.

(H) Confirmation of successful induction of CreER-mediated recombination of *Setd5*$^{LoxP/LoxP}$ allele upon tamoxifen administration by PCR on DNA isolated from tumor biopsy, two independent and representative samples are shown for each treatment group.

(I) Representative HE-stained sections and immunohistochemical staining of pancreas tissue from dual recombinase mouse model of PDAC treated with Tamoxifen, MEKi or placebo (vehicle), (representative of n = 9 mice for each experimental group). Scale bars, 50 μm.

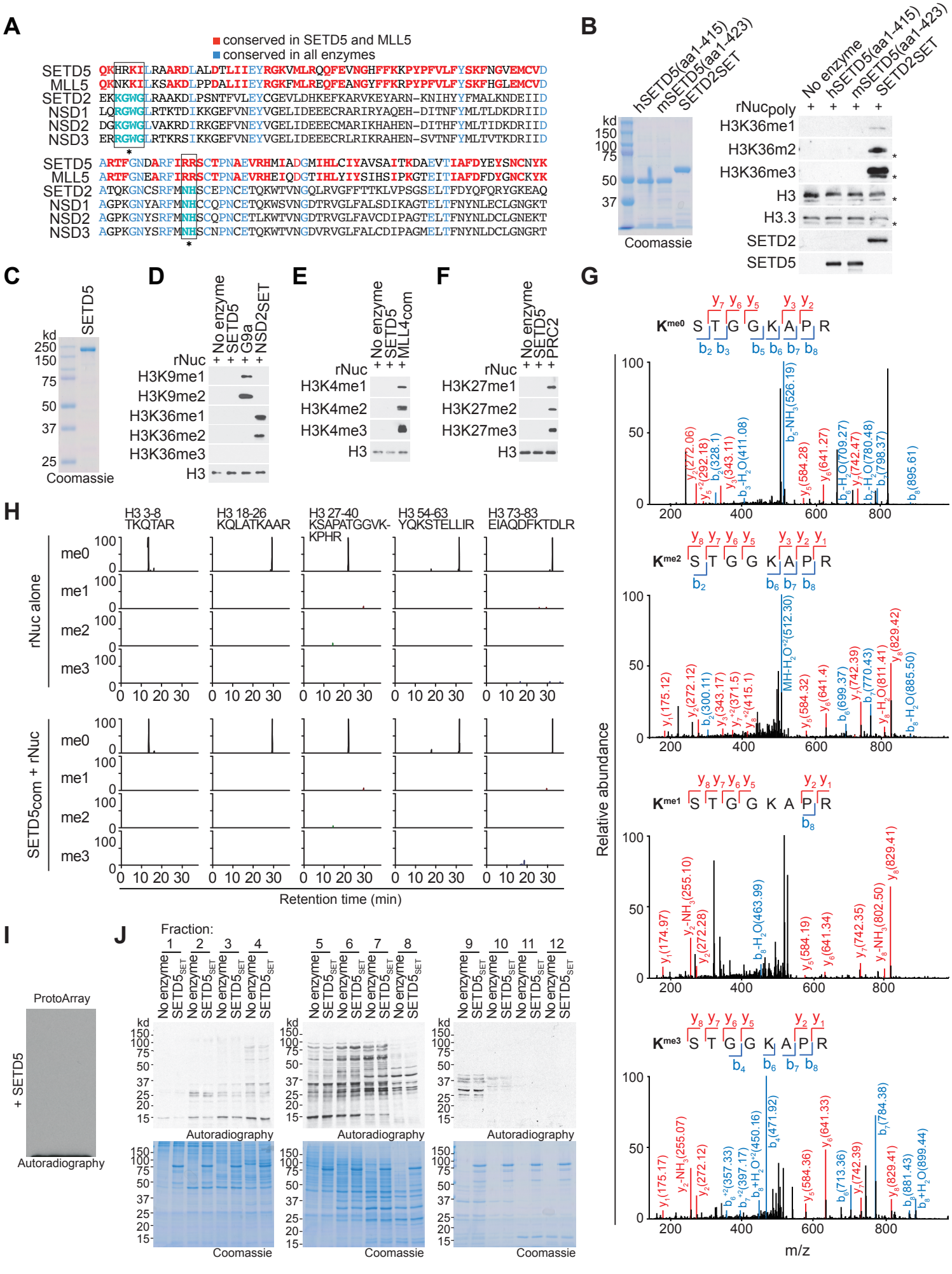
A
conserved in SETD5 and MLL5
conserved in all enzymes
SETD5 QKHRKILRAARDLALDTLIIEYRGKVMLRQQFEVNGHFFKKPYPFVLFYSKFNGVEMCVD
MLL5 QKNKKILKSAKDLPPDALIIEYRGKFMLREQFEANGYFFKRPYPFVLFYSKFHGLEMCVD
SETD2 EKKGWGLRAAKDLPSNTFVLEYCGEVLDHKEFKARVKEYARN-KNIHYYFMALKNDEIID
NSD1 LQRGWGLRTKTDIKKGEFVNEYVGELIDEEECRARIRYAQEH-DITNFYMLTLDKDRIID
NSD2 DGKGWGLVAKRDIRKGEFVNEYVGELIDEEECMARIKHAHEN-DITHFYMLTIDKDRIID
NSD3 ERRGWGLRTKRSIKKGEFVNEYVGELIDEEECRLRIKRAHEN-SVTNFYMLTVTKDRIID
SETD5 ARTFGNDARFIRRSCTPNAEVRHMIADGMIHLCIYAVSAITKDAEVTIAFDYEYSNCNYK
MLL5 ARTFGNEARFIRRSCTPNAEVRHEIQDGTIHLYIYSIHSIPKGTEITIAFDFDYGNCKYK
SETD2 ATQKGNCSRFMNHSCEPNCETQKWTVNGQLRVGFFTTKLVPSGSELTFDYQFQRYGKEAQ
NSD1 AGPKGNYARFMNHCCQPNCETQKWSVNGDTRVGLFALSDIKAGTELTFNYNLECLGNGKT
NSD2 AGPKGNYSRFMNHSCQPNCETLKWTVNGDTRVGLFAVCDIPAGTELTFNYNLDCLGNEKT
NSD3 AGPKGNYSRFMNHSCNPNCETQKWTVNGDVRVGLFALCDIPAGMELTFNYNLDCLGNGRT
B
hSETD5(aa1-415)
mSETD5(aa1-423)
SETD2SET
kd
150
100
75
50
37
Coomassie
No enzyme
hSETD5(aa1-415)
mSETD5(aa1-423)
SETD2SET
rNucpoly + + + +
H3K36me1
H3K36m2
H3K36me3
H3
H3.3
SETD2
SETD5
C
SETD5
kd
250
150
75
50
37
25
Coomassie
D
No enzyme
SETD5
G9a
NSD2SET
rNuc + + + +
H3K9me1
H3K9me2
H3K36me1
H3K36me2
H3K36me3
H3
E
No enzyme
SETD5
MLL4com
rNuc + + +
H3K4me1
H3K4me2
H3K4me3
H3
F
No enzyme
SETD5
PRC2
rNuc + + +
H3K27me1
H3K27me2
H3K27me3
H3
G
Relative abundance
m/z
Kme0 S T G G K A P R
b2 b3 b5 b6 b7 b8
y7 y6 y5 y3 y2
y1(272.06)
y2+2(292.18)
y5
b2(328.1)
y3(343.11)
b3-H2O(411.08)
b5-NH3(526.19)
y5(584.28)
y6(641.27)
b8-H2O(709.27)
y7(742.47)
b2-H2O(780.48)
b2(798.37)
b8(895.61)
Kme2 S T G G K A P R
b2 b6 b7 b8
y8 y7 y6 y5 y3 y2 y1
y1(175.12)
y2(272.12)
b2(300.11)
y3(343.17)
y+2(371.5)
y8+2(415.1)
MH-H2O+2(512.30)
y5(584.32)
y6(641.4)
b8(699.37)
y7(742.39)
b2(770.43)
y8-H2O(811.41)
y8(829.42)
b8-H2O(885.50)
Kme1 S T G G K A P R
b8
y8 y7 y6 y5 y2 y1
y1(174.97)
y2-NH3(255.10)
y2(272.28)
b8-H2O(463.99)
y5(584.19)
y6(641.34)
y7(742.35)
y8-NH3(802.50)
y8(829.41)
Kme3 S T G G K A P R
b4 b6 b7 b8
y8 y7 y6 y5 y2 y1
y1(175.17)
y2-NH3(255.07)
y2(272.12)
b6+2(357.33)
b7+2(397.17)
b8+H2O-2(450.16)
b4(471.92)
y5(584.36)
y6(641.33)
b6(713.36)
y7(742.39)
b7(784.38)
y8(829.41)
b8(881.43)
b8+H2O(899.44)
H
H3 3-8 TKQTAR
H3 18-26 KQLATKAAR
H3 27-40 KSAPATGGVK-KPHR
H3 54-63 YQKSTELLIR
H3 73-83 EIAQDFKTDLR
rNuc alone
SETD5com + rNuc
me0
me1
me2
me3
100
0
0 10 20 30
Retention time (min)
I
ProtoArray
+ SETD5
Autoradiography
J
Fraction:
1 2 3 4 5 6 7 8 9 10 11 12
No enzyme
SETD5SET
kd
150
100
75
50
37
25
20
15
Autoradiography
Coomassie

Supplementary Figure 3. SETD5 lack intrinsic histone methyltransferase activity. Related to Figure 3.

(A) Amino acid sequence alignment of the SET domain of human SETD5 with its most similar family member, the catalytically inert MLL5, and SETD2, NSD1, NSD2 and NSD3 – four validated H3K36 lysine methyltransferases. Boxed and asterisk denoted areas indicated conserved SAM binding sites found within all known active SET enzymes (and not conserved in SETD5 and MLL5).

(B) SETD5 does not methylate H3K36. Coomassie stain of human SETD5 (aa 1-415), murine SETD5 (aa 1-423) and SET domain of SETD2 ($SETD2_{SET}$) purified from *E. coli* (left panel). These proteins were used for *in vitro* methylation reactions with poly-nucleosomes ($rNuc_{poly}$, H3.3) as substrates as described in (Sessa et al., 2019). H3K36me1/2/3 were detected by western blots. Asterisk indicates cleaved H3 found in commercial poly-nucleosome.

(C-F) Full length SETD5 purified from insect cells has no histone methylation activity, in contrast to established KMTs. The purified SETD5 protein from insect cells (C) was used for *in vitro* methylation reactions with recombinant nucleosomes as substrates. Histone methylation states were detected by western blots with the indicated antibodies. SET domain of NSD2 ($NSD2_{SET}$) (D) and MLL4 complex ($MLL4_{com}$) (E) were purified from *E. coli*, PRC2 complex (F) were purified from insect cells.

(G) Representative tandem mass spectra identifying non- (K^{me0}), mono- (K^{me1}), di- (K^{me2}), tri-methylation (K^{me3}) of H3K9 methylated by $SETD5_{com}$ *in vitro* using S-adenosyl-methionine (SAM) as methyl donor and digested with trypsin (as in Figure 3E). *m/z* for b and y ions observed in spectra were indicated in blue and red, respectively.

(H) SETD5 complex has no activity on other histone H3 lysines including no activity on H3K36. Samples (as in F) were analyzed by selected ion chromatograms for non-, mono-, di- and tri-methyl histone H3 peptides. HPLC elution profiles show a 10 ppm mass window around expected peptide masses, peptide sequences flanking potential lysine methylation sites are provided for each panel.

(I) SETD5 does not methylate any protein on a ProtoArray. Representative image (n = 2 independent experiments) showing a SETD5 *in vitro* methylation reaction on protein arrays (ProtoArray - containing more than 9,000 potential substrates) using ^{3}H-SAM as methyl donor. Full length SETD5 was purified from insect cells.

(J) SETD5 does not show any methylation on proteins in nuclear extracts. *In vitro* methylation reactions on nuclear extracts of Panc1 cells separated by size-exclusion chromatography as substrates. $SETD5_{SET}$ (aa 1-520) purified from *E. coli*. was used as enzyme, ^{3}H-SAM as methyl donor. The appearance of a band specific to $SETD5_{SET}$ but not present in the no enzyme control would indicate a potential substrate but such a band is not seen.

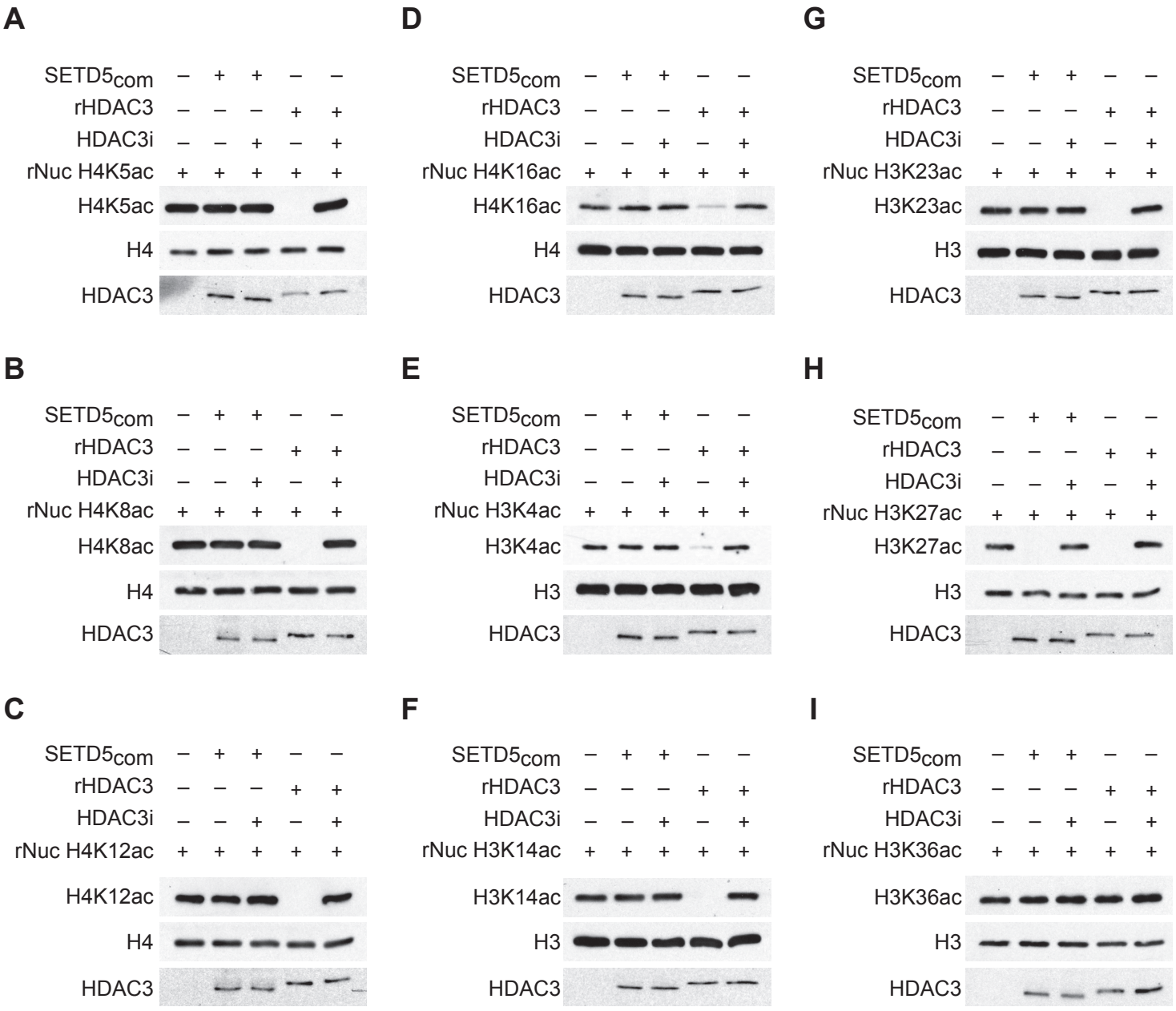
A
SETD5com – + + – –
rHDAC3 – – – + +
HDAC3i – – + – +
rNuc H4K5ac + + + + +
H4K5ac
H4
HDAC3
B
SETD5com – + + – –
rHDAC3 – – – + +
HDAC3i – – + – +
rNuc H4K8ac + + + + +
H4K8ac
H4
HDAC3
C
SETD5com – + + – –
rHDAC3 – – – + +
HDAC3i – – + – +
rNuc H4K12ac + + + + +
H4K12ac
H4
HDAC3
D
SETD5com – + + – –
rHDAC3 – – – + +
HDAC3i – – + – +
rNuc H4K16ac + + + + +
H4K16ac
H4
HDAC3
E
SETD5com – + + – –
rHDAC3 – – – + +
HDAC3i – – + – +
rNuc H3K4ac + + + + +
H3K4ac
H3
HDAC3
F
SETD5com – + + – –
rHDAC3 – – – + +
HDAC3i – – + – +
rNuc H3K14ac + + + + +
H3K14ac
H3
HDAC3
G
SETD5com – + + – –
rHDAC3 – – – + +
HDAC3i – – + – +
rNuc H3K23ac + + + + +
H3K23ac
H3
HDAC3
H
SETD5com – + + – –
rHDAC3 – – – + +
HDAC3i – – + – +
rNuc H3K27ac + + + + +
H3K27ac
H3
HDAC3
I
SETD5com – + + – –
rHDAC3 – – – + +
HDAC3i – – + – +
rNuc H3K36ac + + + + +
H3K36ac
H3
HDAC3

Supplementary Figure 4. HDAC3 is converted into a highly selective deacetylase in the context of SETD5$_{com}$. Related to Figure 5.

(A-I) Screening of histone deacetylation activity of rHDAC3 complex or SETD5$_{com}$ on a library of recombinant nucleosomes designed to harbor a single acetylation modification at specific sites as substrates. Histone acetylation states were detected by western blots with the indicated antibodies: H4K5ac (A), H4K8ac (B), H4K12ac (C), H4K16ac (D), H3K4ac (E), H3K14ac (F), H3K23ac (G), H3K27ac (H) and H3K36a (I). See also Figure 5G-H.

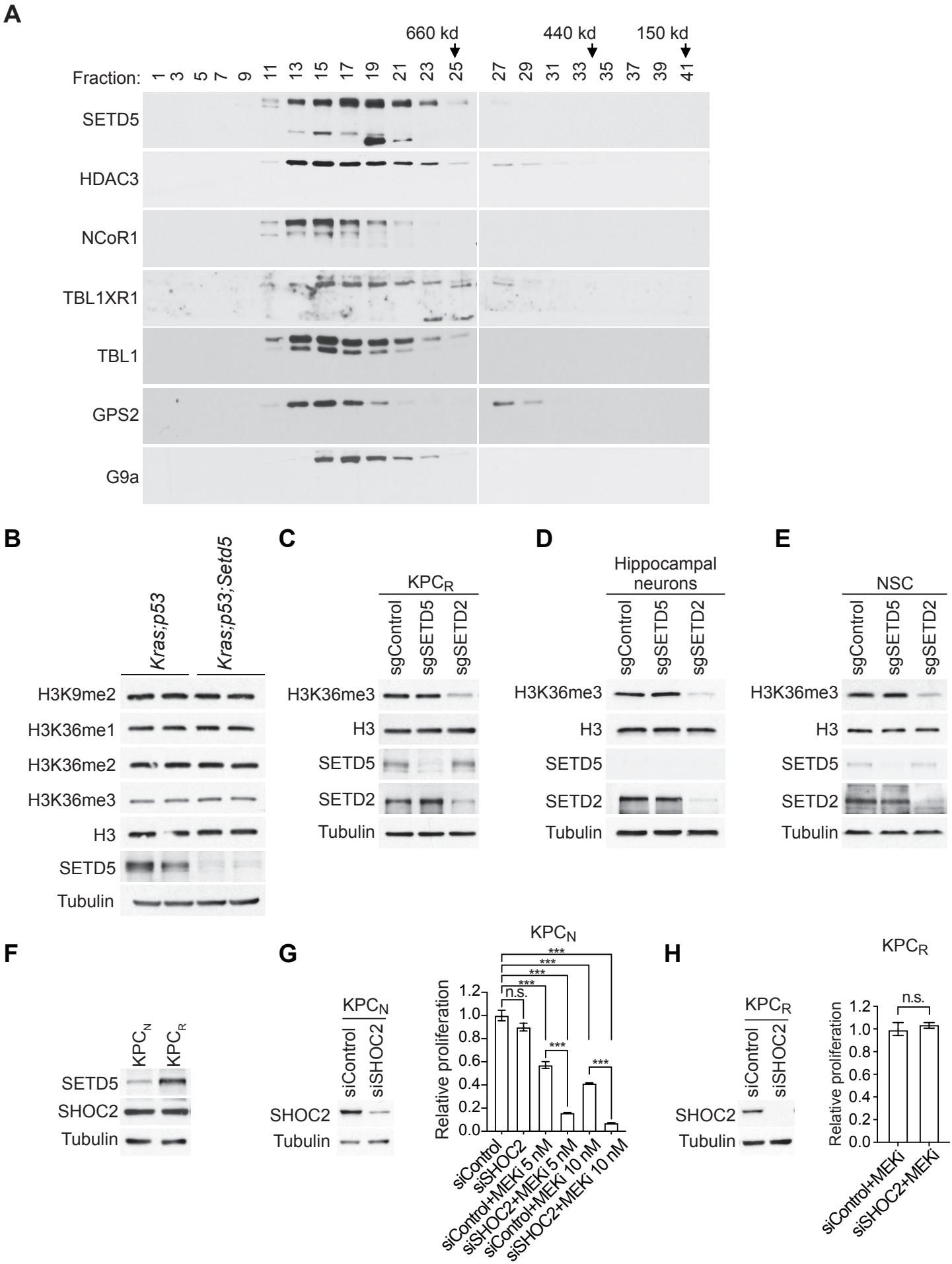
A
660 kd
440 kd
150 kd
Fraction: 1 3 5 7 9 11 13 15 17 19 21 23 25 27 29 31 33 35 37 39 41
SETD5
HDAC3
NCoR1
TBL1XR1
TBL1
GPS2
G9a
B
Kras;p53
Kras;p53;Setd5
H3K9me2
H3K36me1
H3K36me2
H3K36me3
H3
SETD5
Tubulin
C
KPCR
sgControl
sgSETD5
sgSETD2
H3K36me3
H3
SETD5
SETD2
Tubulin
D
Hippocampal neurons
sgControl
sgSETD5
sgSETD2
H3K36me3
H3
SETD5
SETD2
Tubulin
E
NSC
sgControl
sgSETD5
sgSETD2
H3K36me3
H3
SETD5
SETD2
Tubulin
F
KPCN
KPCR
SETD5
SHOC2
Tubulin
G
KPCN
siControl
siSHOC2
SHOC2
Tubulin
KPCN
Relative proliferation
n.s.
***
siControl
siSHOC2
siControl+MEKi 5 nM
siSHOC2+MEKi 5 nM
siControl+MEKi 10 nM
siSHOC2+MEKi 10 nM
H
KPCR
siControl
siSHOC2
SHOC2
Tubulin
KPCR
Relative proliferation
n.s.
siControl+MEKi
siSHOC2+MEKi

Supplementary Figure 5. SETD5 forms a complex with HDAC3 and G9a in KPC_R cells and SETD5 does not physiologically regulate H3K36 methylation. Related to Figure 3 and Figure 6.

(A) Western analysis with the indicated antibodies of $SETD5_{com}$ isolated from KPC_R cell nuclear extracts and separated on a Superose 6 HR gel filtration column. The fraction numbers are indicated and protein molecular mass standards relative to fractions are indicated by arrows.

(B) Western analysis with the indicated antibodies of whole cell lysates of PDAC cells isolated from *Kras;p53* (control) and *Kras;p53;Setd5* mutant mice (see also **Figure S2**). Two independent and representative samples are shown for each genotype. Note that there is no change in H3K36me3 levels.

(C-E) Western analysis with the indicated antibodies of whole cell lysates of KPC_R mouse PDAC cells (C), embryonic hippocampal neurons (D) or neuron stem cells (NSC) (E) depleted using CRISPR-Cas9/sgRNA for SETD5 (sgSETD5), SETD2 (sgSETD2) or control (sgControl). SETD2, a known H3K36me3 methyltransferase serves as positive control of H3K36me3 methylation. A representative sample for each condition is shown. Note that SETD5 depletion has no impact on H3K36 methylation. NSCs were used in Figure 8E in (Sessa et al., 2019).

(F) Western analysis with the indicated antibodies of WCEs from KPC_N and KPC_R cells shows increased levels of SETD5 but not SHOC2 proteins in MEKi-resistant PDAC cells.

(G and H) SHOC2 depletion sensitizes KPCN cells, but not KPCR cells, to MEK inhibition. (G) KPC_N cells treated as indicated with trametinib and (H) KPC_R cells cultured in the presence of 0.2 μM trametinib were transfected with the indicated siRNA pools (siControl and siSHOC2). 48 hours later, a portion of cells was harvested for Western analysis (left panel) and for proliferation assay (right panel), which is shown as relative fold change over siControl. Error bars represent mean ± SD from three independent experiments. ***$p < 0.001$, n.s., not significant, two-tailed unpaired Student's t test.

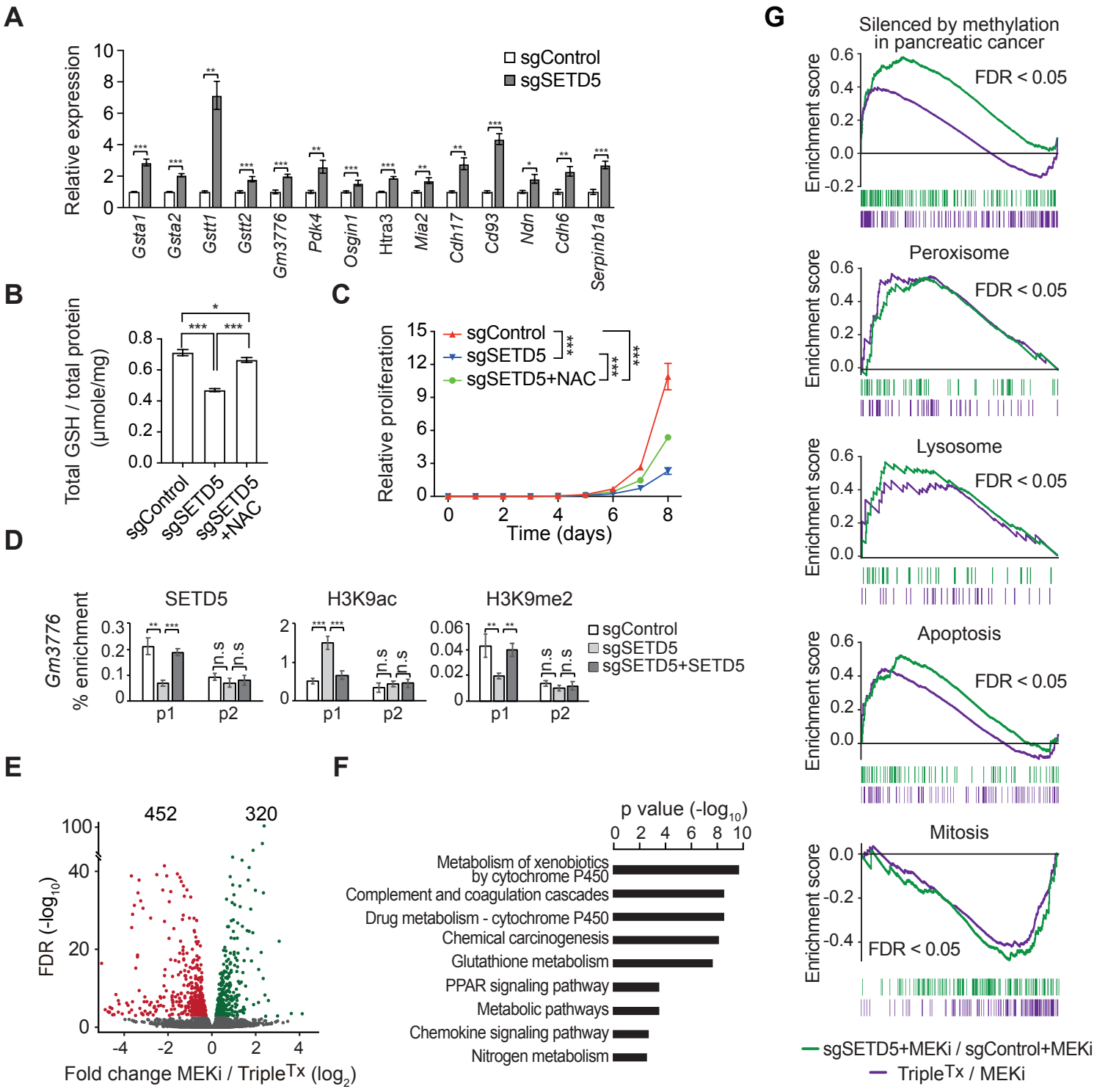
A
Relative expression
sgControl
sgSETD5
Gsta1
Gsta2
Gstt1
Gstt2
Gm3776
Pdk4
Osgin1
Htra3
Mia2
Cdh17
Cd93
Ndn
Cdh6
Serpinb1a
B
Total GSH / total protein (µmole/mg)
sgControl
sgSETD5
sgSETD5 +NAC
C
Relative proliferation
sgControl
sgSETD5
sgSETD5+NAC
Time (days)
D
Gm3776 % enrichment
SETD5
H3K9ac
H3K9me2
sgControl
sgSETD5
sgSETD5+SETD5
p1
p2
n.s
E
452
320
FDR (-log10)
Fold change MEKi / TripleTx (log2)
F
p value (-log10)
Metabolism of xenobiotics by cytochrome P450
Complement and coagulation cascades
Drug metabolism - cytochrome P450
Chemical carcinogenesis
Glutathione metabolism
PPAR signaling pathway
Metabolic pathways
Chemokine signaling pathway
Nitrogen metabolism
G
Silenced by methylation in pancreatic cancer
Peroxisome
Lysosome
Apoptosis
Mitosis
Enrichment score
FDR < 0.05
sgSETD5+MEKi / sgControl+MEKi
TripleTx / MEKi
H
Relative expression
MEKi
TripleTx
Gsta1
Gsta2
Gstt1
Gstt2
Gm3776
Pdk4
Osgin1
Htra3
Mia2
Cdh17
Cd93
Ndn
Cdh6
Serpinb1a
I
sgSETD5 + MEKi
TripleTx
84
9*
311
*p = 1.75-5

Supplementary Figure 6. Small molecule inhibitors of G9a and HDAC3 phenocopy SETD5 loss. Related to Figure 6 and Figure 7.

(A) Quantitative real-time PCR analysis of expression of SETD5 regulated genes in SETD5-deficient (sgSETD5) versus control (sgControl) KPC_R cells. The real-time qPCR data were normalized to *Actb* and presented as fold changes of gene expression. Error bars represent mean ± SD from three independent experiments. *p < 0.05, **p < 0.01, ***p < 0.001, n.s., not significant, by two-tailed unpaired Student's t-test.

(B) N-acetyl-L-Cysteine (NAC) partially restores the levels of GSH in SETD5-depleted KPC_R cells to levels observed in control KPC_R cells. SETD5-depleted KPC_R cells were treated with 1 mM NAC and GSH levels were determined as described in Figure 6H. Error bars represent mean ± SD from three independent experiments. ***p < 0.001, two-tailed unpaired Student's t test.

(C) NAC treatment partially rescues proliferation of SETD5-depleted KPC_R cells to the proliferation rate of control KPC_R cells. Error bars represent mean ± SD from three independent experiments. ***p < 0.001, n.s., not significant, two-tailed unpaired Student's t test.

(D) ChIP-qPCR analysis of SETD5, H3K9ac and H3K9me2 at the *GM3776* (Glutathione S-transferase) gene regulatory regions (*p1* and *p2*) in control (sgControl), SETD5-deficient (sgSETD5) or complemented with CRISPR-resistant wild-type SEDT5 (sgSETD5 + SETD5) KPC_R cells. The data are plotted as percent enrichment relative to input. Error bars represent mean ± SEM from three independent experiments. **p < 0.01, ***p < 0.001, n.s., not significant, by two-tailed unpaired Student's t-test.

(E) Volcano plot representing DEGs (differentially expressed genes) in RNA-seq data comparison between control (MEKi treated) and $Triple^{Tx}$ treated KPC_R cells (three biological replicates for each condition). Detailed cell treatment condition description in **STAR Methods**. The red dots represent 452 upregulated DEGs caused by $Triple^{Tx}$ (fold change $\log_2 \leq -0.5$, $p < 0.05$ by Wald test), green dots represent 320 downregulated DEGs caused by $Triple^{Tx}$ (fold change $\log_2 \geq 0.5$, $p < 0.05$ by Wald test), and grey dots represent non-DEGs. False discovery rate (FDR) values are provided (detailed description in **STAR Methods**).

(F) The most significantly enriched KEGG terms associated with the genes upregulated (452 genes) by $Triple^{Tx}$ treated in KPC_R cancer cells.

(G) GSEA analysis of RNA-seq data of MEKi treated SETD5 ablated (sgSETD5+MEKi) versus control (sgControl+MEKi) and $Triple^{Tx}$ treated versus control (MEKi) KPC_R cells. FDR values are provided (detailed description in **STAR Methods**).

(H) Quantitative real-time PCR analysis of expression of SETD5 regulated genes in $Triple^{Tx}$ versus control (MEKi) KPC_R cancer cell line. The real-time qPCR data were normalized to *Actb* and presented as fold changes of gene expression. Error bars represent mean ± SD from three independent experiments. **p < 0.01, ***p < 0.001, n.s., not significant, by two-tailed unpaired Student's t-test.

(I) Venn diagram showing the overlap between downregulated genes in SETD5 depletion and $Triple^{Tx}$ therapy in MEKi resistant KPC_R cancer cells. p value by hypergeometric test.

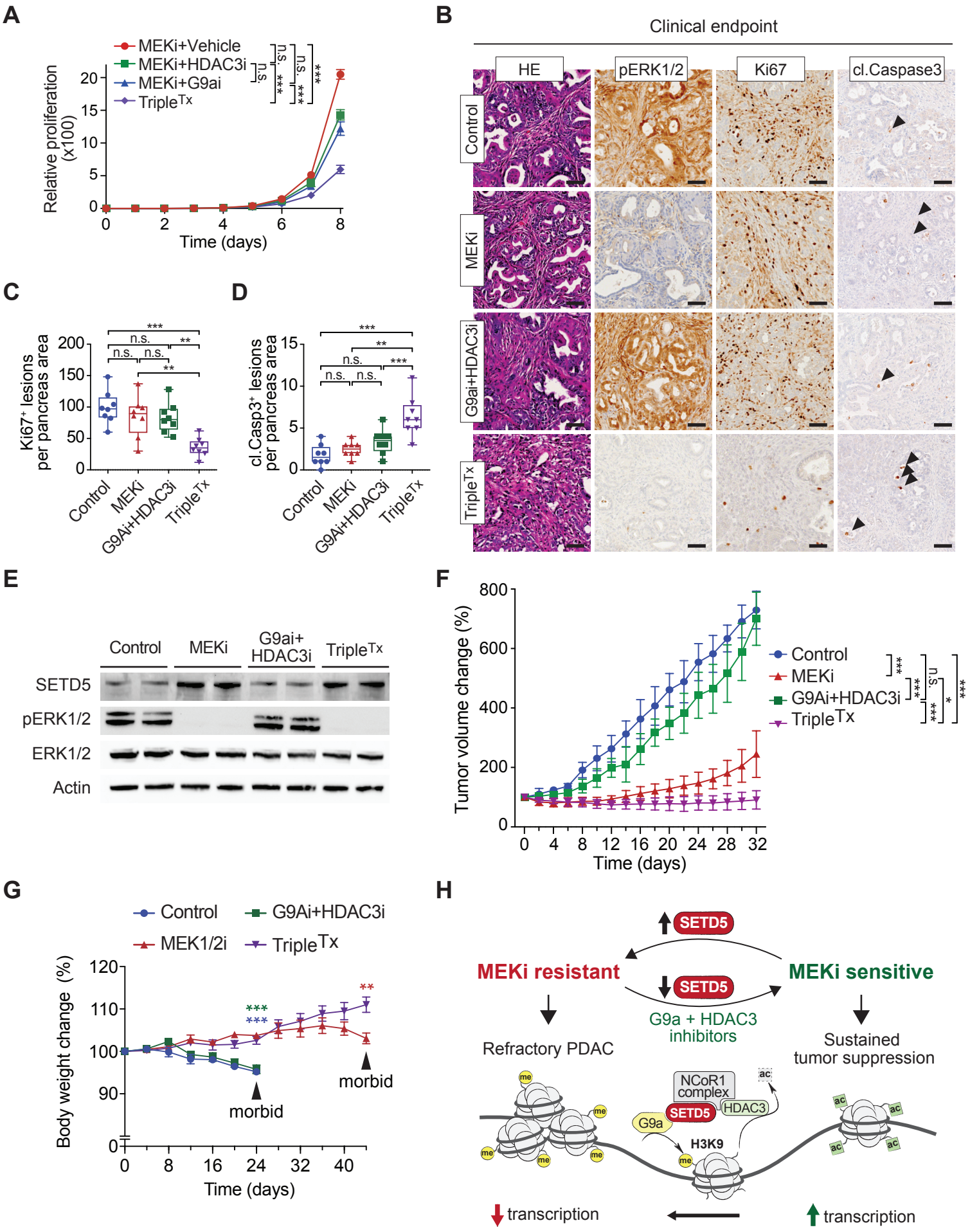
A
MEKi+Vehicle
MEKi+HDAC3i
MEKi+G9ai
Triple^Tx
Relative proliferation (x100)
Time (days)
B
Clinical endpoint
HE
pERK1/2
Ki67
cl.Caspase3
Control
MEKi
G9ai+HDAC3i
Triple^Tx
C
Ki67+ lesions per pancreas area
D
cl.Casp3+ lesions per pancreas area
E
Control
MEKi
G9ai+ HDAC3i
Triple^Tx
SETD5
pERK1/2
ERK1/2
Actin
F
Tumor volume change (%)
Time (days)
G
Control
G9Ai+HDAC3i
MEK1/2i
Triple^Tx
Body weight change (%)
morbid
Time (days)
H
SETD5
MEKi resistant
MEKi sensitive
G9a + HDAC3 inhibitors
Refractory PDAC
Sustained tumor suppression
NCoR1 complex
HDAC3
G9a
H3K9
transcription
transcription

Supplementary Figure 7. Combined inhibition of MEK and the histone-modifying activities associated with SETD5 leads to sustained suppression of PDAC growth in PDXs and mouse models. Related to Figure 7.

(A) Proliferation for eight days of KPC_R cells treated with MEKi, MEKi + G9ai, MEKi + HDAC3i or Triple^{Tx}. Error bars represent SD from three independent experiments. ***p < 0.001, by two-tailed unpaired Student's t-test.

(B) Representative HE and immunohistochemistry staining for phospho ERK1/2 (pERK1/2) a marker of MEK1/2 inhibition, Ki67, a marker of proliferation, cleaved Caspase 3 (cl. Caspase3) a marker of apoptosis (arrowheads), in control and G9ai + HDAC3i, MEKi and combination treated (Triple^{Tx}) *Kras;p53* mutant mouse model of PDAC. Scale bars, 50 μm

(C and D) Quantification of proliferation (Ki67 positive cells) (C) and cleaved Caspase 3 (cl. Caspase3) (D) a marker of apoptosis in *Kras;p53* mutant mice treated with MEKi, G9ai + HDACi or combination (Triple^{Tx}), (n = 8 for each experimental group). Boxes: 25th to 75th percentile, whiskers: min. to max., center: median; arrowheads, positive cleaved Caspase 3 cells; *p < 0.033, **p < 0.002; ***p < 0.0001 by two-way ANOVA with Tukey's testing for multiple comparisons.

(E) Western analysis with indicated antibodies of tumor biopsies from *Kras;p53* mutant mice treated with MEKi, G9ai+HDACi, combination (Triple^{Tx}) or vehicle (control). Each treatment group represents two biological replicates.

(F) Tumor volume quantification for patient derived PDAC xenografts treated with MEKi, G9ai+HDACi, Triple^{Tx} or vehicle (control). (n = 8 mice for each treatment group). Data are represented as mean ± SEM. *p < 0.033, **p < 0.002; ***p < 0.0001 by two-way ANOVA with Tukey's testing for multiple comparisons.

(G) *Kras;p53* mutant mice weight changes in the course of treatment (n = 8, for each experimental condition). Note that control animals lose weight as a consequence of increased tumor burden (cachectic state); arrowheads indicate the last measurements that could be performed on animals in the indicated treatment arm. **p < 0.01; ***p < 0.001; by two-tailed unpaired Student's t-test.

(H) Model of the role SETD5 plays at coordinating histone-modifying activities to regulate a gene expression program that mediates adaptive resistance to MEKi therapy.

Table S2. Identification of SETD5 interactions by mass spectrometry. Related to Figure 3.

V5-SETD5-Flag with PreScission Protease cutting site between V5 and SETD5 was tandem-affinity purified (TAP) from 293T cells with V5 and Flag antibody affinity beads. After elution from beads, material was separated by 10% SDS polyacrylamide gel electrophoresis (SDS-PAGE) and silver stained. Proteins in gel slice of ~170 kd were excised, digested with trypsin and analyzed by mass spectrometry. Contaminant signals were removed and only proteins with 2 or more peptides detected are shown.

Protein IDs	Peptides detected	Sequence length
SET domain-containing protein 5	**12**	**1442**
Histone-lysine N-methyltransferase G9a	**7**	**1210**
Alpha-enolase	3	434
Histone H2A type1-J	3	128
Heterogeneous nuclear ribonucleoproteins A2/B1	2	353
Histone H2B type F-S	2	126
Moesin	2	577
Plastin-2	2	627